

## HYBRID MULTISCALE METHODS I. HYPERBOLIC RELAXATION PROBLEMS\*

GIACOMO DIMARCO<sup>†</sup> AND LORENZO PARESCHI<sup>‡</sup>

**Abstract.** In this paper we consider the development of hybrid numerical methods for the solution of hyperbolic relaxation problems with multiple scales. The main ingredients in the schemes are a suitable merging of probabilistic Monte Carlo methods in non-stiff regimes with high resolution shock capturing techniques in stiff ones. The key aspect in the development of the algorithms is the choice of a suitable hybrid representation of the solution. After the introduction of the different schemes the performance of the new methods is tested in the case of the Jin-Xin relaxation system and the Broadwell model.

**Key words.** multiscale problems, stiff equations, hyperbolic system with relaxation, Monte Carlo methods, shock capturing schemes.

**AMS subject classifications.** 34E13, 35L60, 65C05, 65M99, 82C80

### 1. Introduction

Hyperbolic systems with relaxation are used to describe many physical problems that involve both convection and nonlinear interaction [7, 22]. In the Boltzmann equation from the kinetic theory of rarefied gas dynamics, the collision (relaxation) term describes the interaction of particles [6]. Relaxations also occur in several other problems ranging from water waves to traffic flow. In such systems, when the nonlinear interactions are strong, the relaxation rate is large. In kinetic theory, for example, this occurs when the mean free path between collisions is small (i.e., the Knudsen number is small). Within this regime, which is referred to as the fluid dynamic limit, the gas flow is well described by the Euler or Navier Stokes equations of fluid mechanics, except in shock layers and boundary layers.

These problems represent a challenge for numerical methods due to the presence of different time and/or space scales. In these systems, besides conventional deterministic discretizations, a probabilistic approach is highly desirable. Monte Carlo methods or probabilistic techniques at different levels are widely used to simulate complex systems [3, 21]. They have many advantages in terms of computational cost for problems with high dimensions, simplicity in preserving some physical properties of the underlying problem (typically using a particle interpretation of the statistical sample) and great flexibility when dealing with complicated geometries.

A characteristic of relaxation-like systems is to present a natural dimension reduction of the model due to a large variation of some parameters [7, 22, 17, 24]. Domain decomposition techniques are then used in order to better adapt the modelling strategy and the design of the numerical schemes. However this multi-modelling approach, which at the mathematical level is a consequence of asymptotic approximations, requires the a-priori knowledge of some of the scales in the problem which are typically hard to know in practice [1, 19].

---

\*Received: November 8, 2005; accepted (in revised version): January 11, 2006. Communicated by Shi Jin.

This work was partially supported by the European network HYKE, funded by the EC as contract HPRN-CT-2002-00282 and by the project NUMSTAT funded by the University of Ferrara.

<sup>†</sup>University of Ferrara - Department of Mathematics, Ferrara, Italy (Giacomo.Dimarco@unife.it).

<sup>‡</sup>University of Ferrara - Department of Mathematics, Ferrara, Italy (Lorenzo.Pareschi@unife.it).

A complementary strategy would be to use the full model in the whole computational domain and to design the numerical method in such a way that it is capable of taking advantage of the model reduction induced by the presence of small scales [4, 14, 15, 16, 23, 25]. Of course this would involve the development of heterogeneous numerical methods which hybridize different numerical approaches of probabilistic and deterministic nature.

Often, the design of such hybrid methodology involves not only the use of hybrid numerical methods but also their efficient coupling with suitable multi-modelling strategies. Clearly the details of the schemes are rather problem dependent [5, 8, 26, 27, 18, 30, 31]. We quote the recent works by Weinan E and Bjorn Engquist for a general approach to heterogeneous multiscale methods in scientific computing [10, 11, 12].

In this work we describe a methodology that can be applied to design new hybrid methods for the numerical solution of a wide class of hyperbolic problems that involve different scales. The main components of the schemes is the use of probabilistic Monte Carlo methods for the full model (far from equilibrium regimes) combined with deterministic shock capturing techniques for the reduced one (close to equilibrium regimes). An essential aspect in the development of the algorithms is the choice of a suitable hybrid representation of the solution. The main features of the schemes can be summarized as follows:

- In non stiff regions, where the solution of the full dimensional model is required, the schemes provide a probabilistic Monte Carlo approximation of the solution.
- In stiff regions, where the reduced equilibrium model is valid, the schemes provide a deterministic high order finite volumes (differences) approximation without any time step restrictions induced by the small relaxation rate.
- In intermediate regions, the approximated solution is generated automatically by the schemes as a suitable blending of a nonequilibrium probabilistic component and an equilibrium deterministic component.

The rest of the article is organized as follows. First we introduce the model problems we are considering. Then we present the different schemes in the case of the Jin-Xin relaxation system. Next we apply the method to the more realistic case of the Broadwell model. Some final considerations and future developments are discussed in the last section.

## 2. Hyperbolic relaxation systems

We will consider here one-dimensional hyperbolic systems with relaxation of the form [7]

$$\partial_t U + \partial_x F(U) = \frac{1}{\varepsilon} R(U), \quad x \in \mathbb{R}, \quad (2.1)$$

where  $U = U(x, t) \in \mathbb{R}^N$ ,  $F: \mathbb{R}^N \rightarrow \mathbb{R}^N$ , the Jacobian matrix  $F'(U)$  has real eigenvalues and  $\varepsilon > 0$  is the relaxation time.

The operator  $R: \mathbb{R}^N \rightarrow \mathbb{R}^N$  is said to be a relaxation operator, and consequently (2.1) defines a relaxation system in the sense of Whitham and Liu [22], if there exists a constant  $n \times N$  matrix  $Q$  with  $\text{rank}(Q) = n < N$  such that

$$QR(U) = 0 \quad \forall U \in \mathbb{R}^N. \quad (2.2)$$

This gives  $n$  independent conserved quantities  $v = QU$ . Moreover such conserved

quantities uniquely determine a local equilibrium value

$$U = \mathcal{E}(v) \text{ such that } R(\mathcal{E}(v)) = 0. \quad (2.3)$$

The image of  $\mathcal{E}$  represents the manifold of local equilibria of the relaxation operator  $R$ . Using (2.2) in (2.1) we obtain a system of  $n$  conservation laws which is satisfied by every solution of (2.1)

$$\partial_t(QU) + \partial_x(QF(U)) = 0. \quad (2.4)$$

For small values of the relaxation parameter  $\varepsilon$  from (2.1) we get  $R(U) = 0$  which by (2.3) implies  $U = \mathcal{E}(v)$ . In this case system (2.1) is well approximated by the reduced system

$$\partial_t v + \partial_x G(v) = 0, \quad (2.5)$$

where  $G(v) = QF(\mathcal{E}(v))$ .

**REMARK 2.1.** *Following the terminology introduced in [10, 11, 12] the macroscale process is described by the conserved quantities  $v$  whereas the microscopic process is described by the variables  $U$ . The two processes and state variables are related to each other by compression and reconstruction operators, characterized respectively by the matrices  $Q$  and  $M$  such that  $QU = v$  and  $Mv = U$ , with the property  $QM = I$ , where  $I$  is the  $n$ -dimensional identity matrix. The compression operator is in general a local/ensemble average (projection to low order moments). The reconstruction operator does the opposite and in general it is under-determined, except close to the local equilibrium state when  $R(U) = 0$  implies  $U = \mathcal{E}(v)$ .*

**2.1. Jin-Xin relaxation system.** A simple prototype example of a relaxation system in the case  $N = 2$  is given by the Jin-Xin system [17]

$$\begin{aligned} \partial_t u + \partial_x v &= 0, \\ \partial_t v + \partial_x au &= -\frac{1}{\varepsilon}(v - F(u)), \end{aligned} \quad (2.6)$$

which corresponds to taking  $U = (u, v)^T$ ,  $F(U) = (v, au)^T$  and  $R(U) = (0, F(u) - v)^T$ .

For small values of  $\varepsilon$  from the second equation in (2.6) we get the local equilibrium

$$v = F(u) \quad (2.7)$$

and under Liu's subcharacteristic condition  $a > F'(u)^2$  solutions to (2.6) converges to the solution of the scalar conservation law

$$\partial_t u + \partial_x F(u) = 0. \quad (2.8)$$

**2.2. Broadwell model.** A simple discrete velocity kinetic model for a gas was introduced by Broadwell [2]. It describes a fictitious gas composed of particles with only six (four) velocities in the 3D (2D) velocity space. In one space dimension these models read

$$\begin{aligned} \partial_t f + \partial_x f &= \frac{1}{\varepsilon}(h^2 - fg), \\ \partial_t g - \partial_x g &= \frac{1}{\varepsilon}(h^2 - fg), \\ \partial_t h &= -\frac{1}{\alpha\varepsilon}(h^2 - fg), \end{aligned} \quad (2.9)$$

where  $\varepsilon$  is the mean free path,  $f$ ,  $h$ , and  $g$  denote the mass densities of gas particles with speed 1, 0, and  $-1$ , respectively, and  $\alpha = 1$  for the 2D model and  $\alpha = 2$  for the 3D one. The fluid dynamic moment variables are density  $\varrho$ , momentum  $m$ , and velocity  $u$  defined by

$$\varrho = f + 2\alpha h + g, \quad m = f - g, \quad u = \frac{m}{\varrho}. \quad (2.10)$$

In addition define

$$z = f + g. \quad (2.11)$$

Then the Broadwell equations can be rewritten as

$$\begin{aligned} \partial_t \varrho + \partial_x m &= 0, \\ \partial_t m + \partial_x z &= 0, \\ \partial_t z + \partial_x m &= -\frac{1}{2\alpha^2 \varepsilon} (\varrho^2 + (1 - \alpha^2)z^2 + \alpha^2 m^2 - 2\varrho z). \end{aligned} \quad (2.12)$$

Note that if the fluid variables  $\varrho$ ,  $m$ , and  $z$  are known then  $f$ ,  $g$ , and  $h$  can be recovered as

$$f = \frac{1}{2}(z + m), \quad g = \frac{1}{2}(z - m), \quad h = \frac{1}{2\alpha}(\varrho - z). \quad (2.13)$$

A *local equilibrium* is obtained when the state variables satisfy

$$\varrho^2 + (1 - \alpha^2)z^2 + \alpha^2 m^2 - 2\varrho z = 0, \quad (2.14)$$

which gives

$$z = z_E(\varrho, u) = \begin{cases} \frac{\varrho}{3}(2\sqrt{3u^2 + 1} - 1), & \alpha = 2, \\ \frac{1}{2}\varrho(1 + u^2), & \alpha = 1. \end{cases} \quad (2.15)$$

Thus as  $\varepsilon \rightarrow 0$  one gets the fluid dynamic limit described by the set of Euler equations

$$\begin{aligned} \partial_t \varrho + \partial_x(\varrho u) &= 0, \\ \partial_t(\varrho u) + \partial_x z_E(\varrho, u) &= 0. \end{aligned} \quad (2.16)$$

To the next order, a model Navier-Stokes equation can be derived via the Chapman-Enskog expansion. For a description of the Broadwell model and its fluid dynamic limit see, for example [2].

### 3. Hybrid methods

The starting point in the construction of the methods is the following definition of a hybrid representation of a discrete probability density.

**DEFINITION 3.1.** *Given a discrete probability density  $p_i$ ,  $i = 1, \dots, N$  (i.e.  $p_i \geq 0$ ,  $\sum_i p_i = 1$ ) and a discrete probability density  $E_i$ ,  $i = 1, \dots, N$  called equilibrium density, we define  $w_i \in [0, 1]$  and  $\tilde{p}_i \geq 0$  in the following way*

$$w_i = \begin{cases} \frac{p_i}{E_i}, & p_i \leq E_i \neq 0 \\ 1, & p_i \geq E_i \end{cases} \quad (3.1)$$

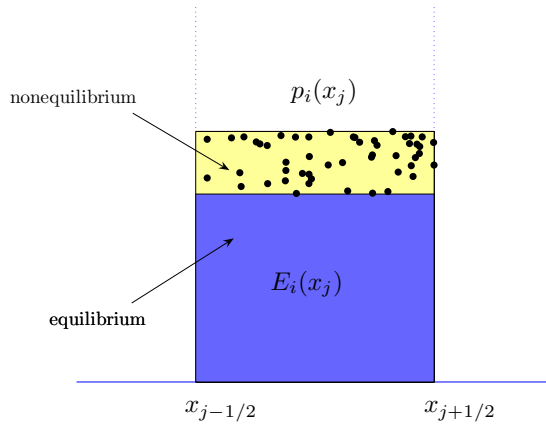


FIG. 2.1. Hybrid representation of a cell value.

and

$$\tilde{p}_i = p_i - w_i E_i. \quad (3.2)$$

Thus  $p_i$  can be represented as

$$p_i = \tilde{p}_i + w_i E_i. \quad (3.3)$$

REMARK 3.1. If we take

$$\beta = \min_i \{w_i\}, \quad (3.4)$$

and

$$\tilde{p}_i = p_i - \beta E_i, \quad (3.5)$$

we have

$$\sum_i \tilde{p}_i = 1 - \beta. \quad (3.6)$$

Let us define for  $\beta \neq 1$  the discrete probability density

$$p_i^p = \frac{\tilde{p}_i}{1 - \beta}.$$

The case  $\beta = 1$  is trivial since it implies  $p_i = E_i$ ,  $i = 1, \dots, N$ . Thus the discrete probability density  $p_i$ ,  $i = 1, \dots, N$  can be written as a convex combination of two probability densities in the form [26, 27]

$$p_i = (1 - \beta)p_i^p + \beta E_i. \quad (3.7)$$

Clearly the above representation is a particular case of (3.3).

In the case of a hyperbolic system with relaxation we recall that  $U(x,t) \in \mathbb{R}^N$  denotes the solution of the system whereas  $\mathcal{E}(v(x,t)) \in \mathbb{R}^N$  denotes the equilibrium state where  $v(x,t) \in \mathbb{R}^n$  are the conserved variables.

Thus we consider the following general representation

$$U(x,t) = \underbrace{\tilde{U}(x,t)}_{\text{nonequilibrium}} + \underbrace{W(x,t)\mathcal{E}(v(x,t))}_{\text{equilibrium}},$$

where  $W(x,t) = \text{diag}(w_1(x,t), w_2(x,t), \dots, w_N(x,t))$ ,  $0 \leq w_i(x,t) \leq 1$  is a  $N \times N$  matrix that characterizes the equilibrium fraction and  $\tilde{U}(x,t)$  the non equilibrium part of the solution.

The general methodology consists of:

- Solving the evolution of the non-equilibrium part by Monte Carlo methods. Thus  $\tilde{U}(x,t)$  will be represented by a set of samples in the computational domain.
- Solving the evolution of the equilibrium part by deterministic methods. Thus  $W(x,t)\mathcal{E}(v(x,t))$  will be represented on a suitable grid in the computational domain.

In the sequel, we will describe the different schemes in the case of the Jin-Xin relaxation system (2.6) although our treatment extends far beyond this simple system. In order to introduce the reader to the main tools used we start the section by describing a simple Monte Carlo approach where the entire solution is represented by samples [29].

**3.1. Monte Carlo methods (MCM).** First we rewrite the system in diagonal form

$$\begin{aligned} \partial_t f + \sqrt{a} \partial_x f &= -\frac{1}{\varepsilon} (f - E_f(u)) \\ \partial_t g - \sqrt{a} \partial_x g &= -\frac{1}{\varepsilon} (g - E_g(u)). \end{aligned}$$

$$f = \frac{\sqrt{a}u + v}{2\sqrt{a}}, \quad g = \frac{\sqrt{a}u - v}{2\sqrt{a}},$$

$$E_f(u) = \frac{\sqrt{a}u + F(u)}{2\sqrt{a}}, \quad E_g(u) = \frac{\sqrt{a}u - F(u)}{2\sqrt{a}}.$$

We assume  $-u\sqrt{a} \leq F(u) \leq u\sqrt{a}$  and  $u \geq 0$  so that  $f, g \geq 0$ . This is guaranteed by the subcharacteristic condition if  $F(0) = 0$ .

We start by splitting the system in the two separate steps, a relaxation step represented by a system of stiff ordinary differential equations

$$\begin{aligned} \partial_t f^r &= -\frac{1}{\varepsilon} (f^r - E_f(u^r)) \\ \partial_t g^r &= -\frac{1}{\varepsilon} (g^r - E_g(u^r)) \end{aligned}$$

and a convection step

$$\begin{aligned} \partial_t f^c + \sqrt{a} \partial_x f^c &= 0 \\ \partial_t g^c - \sqrt{a} \partial_x g^c &= 0. \end{aligned}$$

Note that, given an initial data  $f(x,0)$  and  $g(x,0)$ , we can easily compute the exact solution of the relaxation step as

$$f^r(x,t) = e^{-t/\varepsilon} f(x,0) + (1 - e^{-t/\varepsilon}) E_f(u(x,0)), \tag{3.8}$$

$$g^r(x,t) = e^{-t/\varepsilon} g(x,0) + (1 - e^{-t/\varepsilon}) E_g(u(x,0)). \tag{3.9}$$

This solution is then used as initial data for the transport step to get the approximate solution at time  $t$ . We recall that  $u^r(x,t) = u(x,0)$  during the relaxation step.

In the case of nonnegative initial data and if  $E_f, E_g \geq 0$ , the solution of our problem can be sought in the form of a discrete probability density at each space point

$$p(x,v,t) = \begin{cases} \frac{f(x,t)}{u(x,t)}, & v = \sqrt{a}, \\ \frac{g(x,t)}{u(x,t)}, & v = -\sqrt{a}. \end{cases} \tag{3.10}$$

Let us define with  $\{\nu_1, \nu_2, \dots, \nu_N\}$  the initial samples from  $p(x,v,0)$  at a given space point  $x$ , we know that  $\nu_k = \pm\sqrt{a}$ ,  $k = 1, \dots, N$ . Hence a Monte Carlo method to obtain samples from  $p^r(x,v,t)$  with  $f^r(x,t)$  and  $g^r(x,t)$  solutions of the relaxation step is:

ALGORITHM 3.1 (Simple Monte Carlo for the Jin-Xin relaxation system).

1. Given a sample  $\nu_k$ 
  - (a) with probability  $e^{-t/\varepsilon}$  the sample is unchanged
  - (b) with probability  $1 - e^{-t/\varepsilon}$  the sample is replaced with an equilibrium sample. To extract an equilibrium sample proceed as follows
    - i. with probability  $\frac{E_f(u(x,0))}{u(x,0)}$  take  $\nu_k = \sqrt{a}$
    - ii. with probability  $\frac{E_g(u(x,0))}{u(x,0)}$  take  $\nu_k = -\sqrt{a}$ .

Note that the above procedure requires the exact knowledge of  $u(x,0)$  which we can only estimate from the samples at the given point  $x$ .

In practice we can integrate equations (3.8-3.9) over the cell  $I_j$  and write, up to second order accuracy in space, the time evolution of the cell averages

$$f_{j+1/2}^r(t) = e^{-t/\varepsilon} f_{j+1/2}(0) + (1 - e^{-t/\varepsilon}) E_f(u_{j+1/2}(0)), \tag{3.11}$$

$$g_{j+1/2}^r(t) = e^{-t/\varepsilon} g_{j+1/2}(0) + (1 - e^{-t/\varepsilon}) E_g(u_{j+1/2}(0)). \tag{3.12}$$

Thus we can apply Algorithm 3.1 to the whole set of samples in the space interval associated by the reconstruction of  $u_{j+1/2}(0)$ . The simplest method, which produces a piecewise constant reconstruction, is based on evaluating the histogram of the samples on the grid. Given a set of  $N$  samples  $p_1, p_2, \dots, p_N$  we define the discrete probability density at the cell centers

$$p(x_{j+1/2}) = \frac{1}{N} \sum_{k=1}^N \Psi_{\Delta x}(p_k - x_{j+1/2}), \quad j = \dots, -2, -1, 0, 1, 2, \dots \tag{3.13}$$

where  $\Psi_{\Delta x}(x) = 1/\Delta x$  if  $|x| \leq \Delta x/2$  and  $\Psi_{\Delta x}(x) = 0$  elsewhere.

Let us denote by the index  $k$  the sample  $\nu_k$  and its position  $\chi_k$ . If we use equations (3.13) then  $u_{j+1/2}$  is given by the number of samples  $N_j$  belonging to the cell  $I_j$

$$u_{j+1/2} = \frac{1}{N\Delta x} \sum_{\chi_k \in I_j} 1 = \frac{N_j}{N\Delta x}$$

and the Monte Carlo procedure is applied to such a set of samples  $\{\nu_k | \chi_k \in I_j\}$ . In this case, when we extract a new equilibrium sample  $\nu_k$  in the cell  $I_j$  its position  $\chi_k$  is taken as uniformly distributed in the cell. We refer the reader to [28] (and the references therein) for an introduction to basic sampling and different reconstruction techniques with Monte Carlo methods.

Finally the transport step does not present any difficulty and can be applied without any need of meshes or reconstructions. In fact, from the exact expression of the solution  $f^c(x, t) = f^r(x - \sqrt{at}, t)$ ,  $g^c(x, t) = g^r(x + \sqrt{at}, t)$  we simply need to shift the position of the samples according to the law

$$\chi_k = \chi_k + \nu_k t, \quad \forall k. \quad (3.14)$$

In the sequel we will use the terminology ‘‘particle’’ to denote the pair  $(\chi_k, \nu_k)$  characterizing the sample  $\nu_k$  and its position  $\chi_k$ .

The method described above deserves some remarks.

REMARK 3.2.

- *One important aspect of the method is that we do not need to reconstruct the functions  $f$  and  $g$  but only the conserved quantity  $u$ . This is of paramount relevance when dealing with very large systems, as in kinetic equations.*
- *The Monte Carlo scheme is conservative and preserves positivity of the solution without any time step limitation. Note that as  $\varepsilon \rightarrow 0$  the method becomes a Monte Carlo algorithm for the limiting scalar conservation law. This limiting method is the analogue of a kinetic particle method for the scalar conservation law [29].*
- *The simple splitting method we have described here is first order in time. Second order Strang splitting can be implemented similarly.*

**3.2. The hybrid method (HM).** The standard hybrid method is based on the hybrid representation (3.7). Thus we assume our solution with the form

$$f(x, t) = (1 - \beta(x, t))f_p(x, t) + \beta(x, t)E_f(u(x, t)), \quad (3.15)$$

$$g(x, t) = (1 - \beta(x, t))g_p(x, t) + \beta(x, t)E_g(u(x, t)). \quad (3.16)$$

From the exact solution of the relaxation step (3.8) if we consider that initially

$$\begin{aligned} f(x, 0) &= (1 - \beta(x, 0))f_p(x, 0) + \beta(x, 0)E_f(u(x, 0)), \\ g(x, 0) &= (1 - \beta(x, 0))g_p(x, 0) + \beta(x, 0)E_g(u(x, 0)) \end{aligned}$$

we obtain the identities

$$\begin{aligned} f^r(x, t) &= (1 - \beta^r(x, t))f_p^r(x, t) + \beta^r(x, t)E_f(u^r(x, t)) \\ &= e^{-t/\varepsilon}[(1 - \beta(x, 0))f_p(x, 0) + \beta(x, 0)E_f(u(x, 0))] + \\ &\quad + (1 - e^{-t/\varepsilon})E_f(u(x, 0)), \\ g^r(x, t) &= (1 - \beta^r(x, t))g_p^r(x, t) + \beta^r(x, t)E_g(u^r(x, t)) \\ &= e^{-t/\varepsilon}[(1 - \beta(x, 0))g_p(x, 0) + \beta(x, 0)E_g(u(x, 0))] + \\ &\quad + (1 - e^{-t/\varepsilon})E_g(u(x, 0)). \end{aligned}$$

By equating the equilibrium terms and the non equilibrium ones in the above equations and using the fact that  $u^r(x, t) = u(x, 0)$  we obtain the evolution for the unknowns

$f_p^r(x,t)$ ,  $g_p^r(x,t)$  and  $\beta^r(x,t)$

$$f_p^r(x,t) = f_p(x,0), \quad g_p^r(x,t) = g_p(x,0). \quad (3.17)$$

$$\beta^r(x,t) = e^{-t/\varepsilon} \beta(x,0) + 1 - e^{-t/\varepsilon}. \quad (3.18)$$

Note that  $\beta^r(x,t) \rightarrow 1$  as  $\varepsilon \rightarrow 0$ . If we start from  $\beta(x,0) = 0$  (all particles) at the end of the relaxation a fraction  $1 - e^{-t/\varepsilon}$  of the particles is discarded by the method as the effect of the relaxation to equilibrium. Thus particles will represent the fractions  $(1 - \beta^r(x,t))f_p^r(x,t)$  and  $(1 - \beta^r(x,t))g_p^r(x,t)$ . Moreover the hybrid representation is naturally kept by the relaxation.

After relaxation the exact solution of the transport step reads

$$\begin{aligned} f^c(x,t) &= (1 - \beta^c(x,t))f_p^c(x,t) + \beta^c(x,t)E_f(u^c(x,t)) = f^r(x - \sqrt{at}, t) \\ &= (1 - \beta^r(x - \sqrt{at}, t))f_p^r(x - \sqrt{at}, t) + \\ &\quad + \beta^r(x - \sqrt{at}, t)E_f(u(x - \sqrt{at}, 0)) \\ g^c(x,t) &= (1 - \beta^c(x,t))g_p^c(x,t) + \beta^c(x,t)E_g(u^c(x,t)) = g^r(x + \sqrt{at}, t) \\ &= (1 - \beta^r(x + \sqrt{at}, t))g_p^r(x + \sqrt{at}, t) + \\ &\quad + \beta^r(x + \sqrt{at}, t)E_g(u(x + \sqrt{at}, 0)). \end{aligned} \quad (3.19)$$

To simplify notations let us set

$$\begin{aligned} f_p^*(x,t) &= (1 - \beta^r(x - \sqrt{at}, t))f_p^r(x - \sqrt{at}, t), \\ E_f^*(x,t) &= \beta^r(x - \sqrt{at}, t)E_f(u(x - \sqrt{at}, 0)), \\ g_p^*(x,t) &= (1 - \beta^r(x + \sqrt{at}, t))g_p^r(x + \sqrt{at}, t), \\ E_g^*(x,t) &= \beta^r(x + \sqrt{at}, t)E_g(u(x + \sqrt{at}, 0)). \end{aligned}$$

Unfortunately now the hybrid structure of the solution is not kept since  $E_f^*(x,t)$  and  $E_g^*(x,t)$  are not equilibrium states. For example the above set of equations can be solved taking

$$\beta^c(x,t) = 0, \quad (3.20)$$

and

$$f^c(x,t) = f_p^*(x,t) + E_f^*(x,t), \quad (3.21)$$

$$g^c(x,t) = g_p^*(x,t) + E_g^*(x,t). \quad (3.22)$$

Thus we need to resample the whole deterministic fraction  $E_f^*(x,t)$  and  $E_g^*(x,t)$ .

Note however that if we move one step  $t_1$  further in the relaxation using  $f^c(x,t)$  and  $g^c(x,t)$  defined above as initial data we have  $\beta^r(x, t+t_1) = 1 - e^{-t_1/\varepsilon}$  and

$$\begin{aligned} f^r(x, t+t_1) &= (1 - \beta^r(x, t+t_1))f_p^r(x, t+t_1) + \\ &\quad + \beta^r(x, t+t_1)E_f(u^r(x, t+t_1)) \\ &= e^{-t_1/\varepsilon} f^c(x, t) + (1 - e^{-t_1/\varepsilon})E_f(u^c(x, t)) \\ &= e^{-t_1/\varepsilon} (f_p^*(x, t) + E_f^*(x, t)) + (1 - e^{-t_1/\varepsilon})E_f(u^c(x, t)), \end{aligned} \quad (3.23)$$

$$\begin{aligned} g^r(x, t+t_1) &= (1 - \beta^r(x, t+t_1))g_p^r(x, t+t_1) + \\ &\quad + \beta^r(x, t+t_1)E_g(u^r(x, t+t_1)) \\ &= e^{-t_1/\varepsilon} g^c(x, t) + (1 - e^{-t_1/\varepsilon})E_g(u^c(x, t)) \\ &= e^{-t_1/\varepsilon} (g_p^*(x, t) + E_g^*(x, t)) + (1 - e^{-t_1/\varepsilon})E_g(u^c(x, t)). \end{aligned} \quad (3.24)$$

Thus, in practice, we can avoid resampling particles after the convection and apply the resampling only on a fraction  $e^{-t_1/\varepsilon}$  of the deterministic fraction as needed by the relaxation. More precisely taking cell averages of (3.23)-(3.24) as in a standard Monte Carlo method, and using equations (3.13) for the reconstruction as shown later, the algorithm to compute the particles that represent the fractions  $e^{-t_1/\varepsilon} f_{j+1/2}^c(t)$  and  $e^{-t_1/\varepsilon} g_{j+1/2}^c(t)$  reads as follows:

ALGORITHM 3.2 (Hybrid Monte Carlo for Jin-Xin relaxation).

1. Given  $m = \frac{\Delta x}{N} \sum_j u_{j+1/2}^c(t)$
2. for each interval  $I_j$ ,  $j = \dots, -2, -1, 0, 1, 2, \dots$ 
  - (a) set  $\beta_j = 1 - e^{-t_1/\varepsilon}$
  - (b) set  $N_j = \text{Iround} \left( (1 - \beta_j) \frac{\Delta x}{m} u_{j+1/2}^c(t) \right)$
  - (c) set  $P_j = \frac{u_{p,j+1/2}^*(t)}{u_{p,j+1/2}^*(t) + u_{E,j+1/2}^*(t)}$ ,  
with  $u_{p,j+1/2}^*(t) = f_{p,j+1/2}^*(t) + g_{p,j+1/2}^*(t)$   
and  $u_{E,j+1/2}^*(t) = E_{f,j+1/2}^*(t) + E_{g,j+1/2}^*(t)$
  - (d) for  $k = 1, \dots, N_j$   
with probability  $P_j$  take  $(\nu_k, \chi_k)$  as one of the advected particles.  
with probability  $1 - P_j$  take one sample  $\nu_k$  from the deterministic fraction. To extract such a sample do the following
    - i. with probability  $\frac{E_{f,j+1/2}^*(t)}{u_{E,j+1/2}^*(t)}$  take  $\nu_k = \sqrt{a}$
    - ii. with probability  $\frac{E_{g,j+1/2}^*(t)}{u_{E,j+1/2}^*(t)}$  take  $\nu_k = -\sqrt{a}$
    - iii. take  $\chi_k$  uniformly distributed in  $I_j$ .

After this the hybrid solution is computed simply adding the deterministic terms

$$\beta_j E_f(u_{j+1/2}^c(t)), \quad \beta_j E_g(u_{j+1/2}^c(t))$$

to the stochastic terms

$$(1 - \beta_j) f_{p,j+1/2}^r(t) = \frac{m}{\Delta x} N_j^+, \quad (1 - \beta_j) g_{p,j+1/2}^r(t) = \frac{m}{\Delta x} N_j^-$$

where  $N_j^+$  and  $N_j^-$  are the number of samples in cell  $I_j$  equal to  $\sqrt{a}$  and  $-\sqrt{a}$  respectively.

This permits us to avoid inefficient discard-resample procedures for small values of  $\varepsilon$ . For example, as  $\varepsilon \rightarrow 0$  we do not perform any resampling at all, and we obtain a relaxation scheme for the limiting scalar conservation law.

REMARK 3.3.

- The convection part corresponding to  $f_p^*(x, t)$  and  $g_p^*(x, t)$  is solved exactly by the transport of particles as in a full Monte Carlo method. Instead the convection part corresponding to  $E_f^*(x, t)$  and  $E_g^*(x, t)$  can be solved by finite volumes or finite differences since it corresponds to solving the convection step with initial data  $f(x, 0) = \beta^r(x, t) E_f(u(x, 0))$  and  $g(x, 0) = \beta^r(x, t) E_g(u(x, 0))$ .
- In contrast to the simple Monte Carlo method positivity of the hybrid solution and presence of time step restrictions depend on the deterministic scheme used to solve the convection part for  $E_f^*(x, t)$  and  $E_g^*(x, t)$ .

- Note that the effective value of  $\beta_j$  used in the above algorithm differs from  $1 - e^{-t_1/\varepsilon}$ . In fact if  $N_j^c$  denotes the number of particles in cell  $j$  after the convection step, during the relaxation we keep only an integer approximation  $N_j^\beta$  of  $(1 - \beta_j)N_j^c$ . The effective value of  $\beta_j$  can then be computed at the end of the algorithm as

$$\beta_j^E = 1 - \frac{N_j^\beta}{N_j^c}.$$

**3.3. A Componentwise hybrid method (CHM).** A better approach would consist in finding the maximum value of  $\beta^c(x, t) > 0$  in order to maximize the deterministic fraction in equations (3.19). In order to achieve this goal we consider the componentwise hybrid representation

$$f(x, t) = \tilde{f}(x, t) + w_f(x, t)E_f(u(x, t)), \quad (3.25)$$

$$g(x, t) = \tilde{g}(x, t) + w_g(x, t)E_g(u(x, t)). \quad (3.26)$$

The relaxation step now leads to

$$\begin{aligned} f^r(x, t) &= \tilde{f}^r(x, t) + w_f^r(x, t)E_f(u^r(x, t)) \\ &= e^{-t/\varepsilon}[\tilde{f}(x, 0) + w_f(x, 0)E_f(u(x, 0))] + \\ &\quad + (1 - e^{-t/\varepsilon})E_f(u(x, 0)), \\ g^r(x, t) &= \tilde{g}^r(x, t) + w_g^r(x, t)E_g(u^r(x, t)) \\ &= e^{-t/\varepsilon}[\tilde{g}(x, 0) + w_g(x, 0)E_g(u(x, 0))] + \\ &\quad + (1 - e^{-t/\varepsilon})E_g(u(x, 0)). \end{aligned}$$

Again by equating the equilibrium terms and the non equilibrium ones in the above equations we obtain the evolution for the unknowns  $\tilde{f}^r(x, t)$ ,  $\tilde{g}^r(x, t)$ ,  $w_f^r(x, t)$  and  $w_g^r(x, t)$

$$\tilde{f}^r(x, t) = e^{-t/\varepsilon}\tilde{f}(x, 0), \quad w_f^r(x, t) = e^{-t/\varepsilon}w_f(x, 0) + 1 - e^{-t/\varepsilon}, \quad (3.27)$$

$$\tilde{g}^r(x, t) = e^{-t/\varepsilon}\tilde{g}(x, 0), \quad w_g^r(x, t) = e^{-t/\varepsilon}w_g(x, 0) + 1 - e^{-t/\varepsilon}. \quad (3.28)$$

As before the hybrid representation is kept by the relaxation process. The only difference with respect to the HM method is that we discard particles from  $f$  and  $g$  with different ratios.

The convection destroys the structure of the solution and we get

$$\begin{aligned} f^c(x, t) &= \tilde{f}^c(x, t) + w_f^c(x, t)E_f(u^c(x, t)) = f^r(x - \sqrt{at}, t) \\ &= \tilde{f}^r(x - \sqrt{at}, t) + w_f^r(x - \sqrt{at}, t)E_f(u(x - \sqrt{at}, 0)) \end{aligned} \quad (3.29)$$

$$\begin{aligned} g^c(x, t) &= \tilde{g}^c(x, t) + w_g^c(x, t)E_g(u^c(x, t)) = g^r(x + \sqrt{at}, t) \\ &= \tilde{g}^r(x + \sqrt{at}, t) + w_g^r(x + \sqrt{at}, t)E_g(u(x + \sqrt{at}, 0)). \end{aligned} \quad (3.30)$$

To simplify notations let us set

$$\begin{aligned} f_p^*(x, t) &= \tilde{f}^r(x - \sqrt{at}, t), & \tilde{E}_f(x, t) &= w_f^r(x - \sqrt{at}, t)E_f(u(x - \sqrt{at}, 0)), \\ g_p^*(x, t) &= \tilde{g}^r(x + \sqrt{at}, t), & \tilde{E}_g(x, t) &= w_g^r(x + \sqrt{at}, t)E_g(u(x + \sqrt{at}, 0)). \end{aligned}$$

Here we do not assume  $w_f^c(x, t) = 0$ ,  $w_g^c(x, t) = 0$  since we want to take advantage of the componentwise hybrid representation in order to maximize the deterministic fraction of the solution. Thus, starting from the deterministic fractions  $\tilde{E}_f(x, t)$  and  $\tilde{E}_g(x, t)$  defined above we construct the new values of  $w_f^c(x, t)$ ,  $\tilde{f}^c(x, t)$ ,  $w_g^c(x, t)$  and  $\tilde{g}^c(x, t)$  using Definition 3.1.

More precisely we define

$$w_f^c(x, t) = \begin{cases} \frac{\tilde{E}_f(x, t)}{E_f(u^c(x, t))}, & \tilde{E}_f(x, t) \leq E_f(u^c(x, t)) \neq 0 \\ 1, & \tilde{E}_f(x, t) \geq E_f(u^c(x, t)) \end{cases} \quad (3.31)$$

and

$$E_f^*(x, t) = \tilde{E}_f(x, t) - w_f^c(x, t)E_f(u^c(x, t)). \quad (3.32)$$

In this way we obtain

$$\tilde{f}^c(x, t) = f_p^*(x, t) + E_f^*(x, t). \quad (3.33)$$

Note that if  $\tilde{E}_f(x, t) \leq E_f(u^c(x, t)) \neq 0$  we have  $\tilde{f}^c(x, t) = f_p^*(x, t)$  and thus we keep all of the deterministic fraction. Similarly we compute  $w_g^c(x, t)$  and  $\tilde{g}_p^c(x, t)$ .

The next relaxation step then applies straightforwardly using directly Algorithm 3.2 on cell averages. In fact moving one step further we have

$$\begin{aligned} f^r(x, t + t_1) &= \tilde{f}^r(x, t + t_1) + w_f^r(x, t + t_1)E_f(u^r(x, t + t_1)) \\ &= e^{-t_1/\varepsilon} f^c(x, t) + (1 - e^{-t_1/\varepsilon})E_f(u^c(x, t)) \\ &= e^{-t_1/\varepsilon} (f_p^*(x, t) + E_f^*(x, t) + w_f(x, t)E_f(x, t)) + \\ &\quad + (1 - e^{-t_1/\varepsilon})E_f(u^c(x, t)) \end{aligned} \quad (3.34)$$

$$\begin{aligned} g^r(x, t + t_1) &= \tilde{g}^r(x, t + t_1) + w_g^r(x, t + t_1)E_g(u^r(x, t + t_1)) \\ &= e^{-t_1/\varepsilon} g^c(x, t) + (1 - e^{-t_1/\varepsilon})E_g(u^c(x, t)) \\ &= e^{-t_1/\varepsilon} (g_p^*(x, t) + E_g^*(x, t) + w_g(x, t)E_g(x, t)) + \\ &\quad + (1 - e^{-t_1/\varepsilon})E_g(u^c(x, t)). \end{aligned} \quad (3.35)$$

The only difference is that now the final hybrid solution is recovered adding the deterministic terms

$$((1 - \beta_j)w_f(x_{j+1/2}, t) + \beta_j)E_f(u_{j+1/2}^c(t)),$$

$$((1 - \beta_j)w_g(x_{j+1/2}, t) + \beta_j)E_g(u_{j+1/2}^c(t))$$

in each cell.

REMARK 3.4. *If we define after the convection step*

$$\beta^c(x, t) = \min\{w_f^c(x, t), w_g^c(x, t)\}, \quad (3.36)$$

*we maximize the common value of  $\beta^c$  such that the standard hybrid method applies. This is particularly relevant in many applications where it is important that the hybrid decomposition is component independent, for example, for more general relaxation terms.*

#### 4. Implementation and numerical tests

In this section we report some numerical results for the different schemes considered. We use the shorthand MCM, HM1, HM2 and CHM to denote the Monte Carlo Method, the Hybrid Method with the choices (3.20) and (3.36) respectively, and the Componentwise Hybrid Method.

**4.1. High resolution scheme for the equilibrium component.** In order to compute the evolution of the deterministic part of the solution in all the hybrid methods we use a second order MUSCL type scheme based on cell averages [20]. The second order scheme is defined taking as a flux

$$F_j(x_i) = \frac{f_j(x_{i-j+2}) - f_j(x_{i-j+1})}{\Delta x} \phi(\theta_j(x_i)) \quad (4.1)$$

where  $\phi_j$  is the limiter function

$$\phi_j = \phi(\theta_j), \quad \theta_j(x_i) = \left[ \frac{f_j(x_i) - f_j(x_{i-1})}{f_j(x_{i+1}) - f_j(x_i)} \right]^{i_j}.$$

For example the so-called "superbee" of Roe

$$\phi(\theta) = \max(0, \min(1, 2\theta), \min(\theta, 2)).$$

Finally the scheme for the convection step is defined as

$$\begin{aligned} f_j^{n+1/2}(x_i) &= f_j^n(x_i) + \eta(f_j^n(x_{i+i_j}) - f_j^n(x_i)) - \\ &+ i_j \frac{\eta(1-\eta)}{2} [F_j^n(x_{i+i_j})\Delta x - F_j^n(x_{i_j})\Delta x], \quad j=1,2 \end{aligned} \quad (4.2)$$

where  $\eta = \frac{\Delta t}{\Delta x}$  and  $i_j = (-1)^j$ . As  $\varepsilon \rightarrow 0$  the relaxation step becomes a projection step and thus we obtain a second order in space, first order in the time relaxation scheme [17] for the limiting scalar conservation law. Extension to the multidimensional case can be done as usual dimension by dimension.

**4.2. Jin-Xin system.** In all tests we take initially the solution represented by samples and  $F(u) = u^2/2$  (thus as  $\varepsilon \rightarrow 0$  we have the Burgers equation). We consider the following test cases with periodic boundary conditions.

**4.2.1. 1D case.** First we consider a one-dimensional test problem with initial data

$$u(x,0) = \frac{1}{4}(2 + \sin(2\pi x) - \sin(\pi x)), \quad x \in [-1, 1], \quad t \in [0, 1]. \quad (4.3)$$

We report the numerical solution for different values of the relaxation parameter  $\varepsilon = 0.1, 0.01, 0.001$  with 200 grid points starting initially with  $N = 10^3$  particles. The particle solution has been reconstructed using the simple formula (3.13). The final computing times are given in the figures captions (see Figure 4.1 and Figure 4.2). We also compute the  $L_1$  norm of the error in time using a finite difference solution on a very fine mesh (six times the mesh of the methods) as a reference result (see Figure 4.3).

In the same figure the number of particles as a function of time is also given. The variance reduction of hybrid methods with respect to standard MCM is evident. In particular HM2 and CHM have the better efficiency and accuracy properties (note that the results of these two methods are very similar for  $\varepsilon = 0.01$  and  $\varepsilon = 0.001$ ).

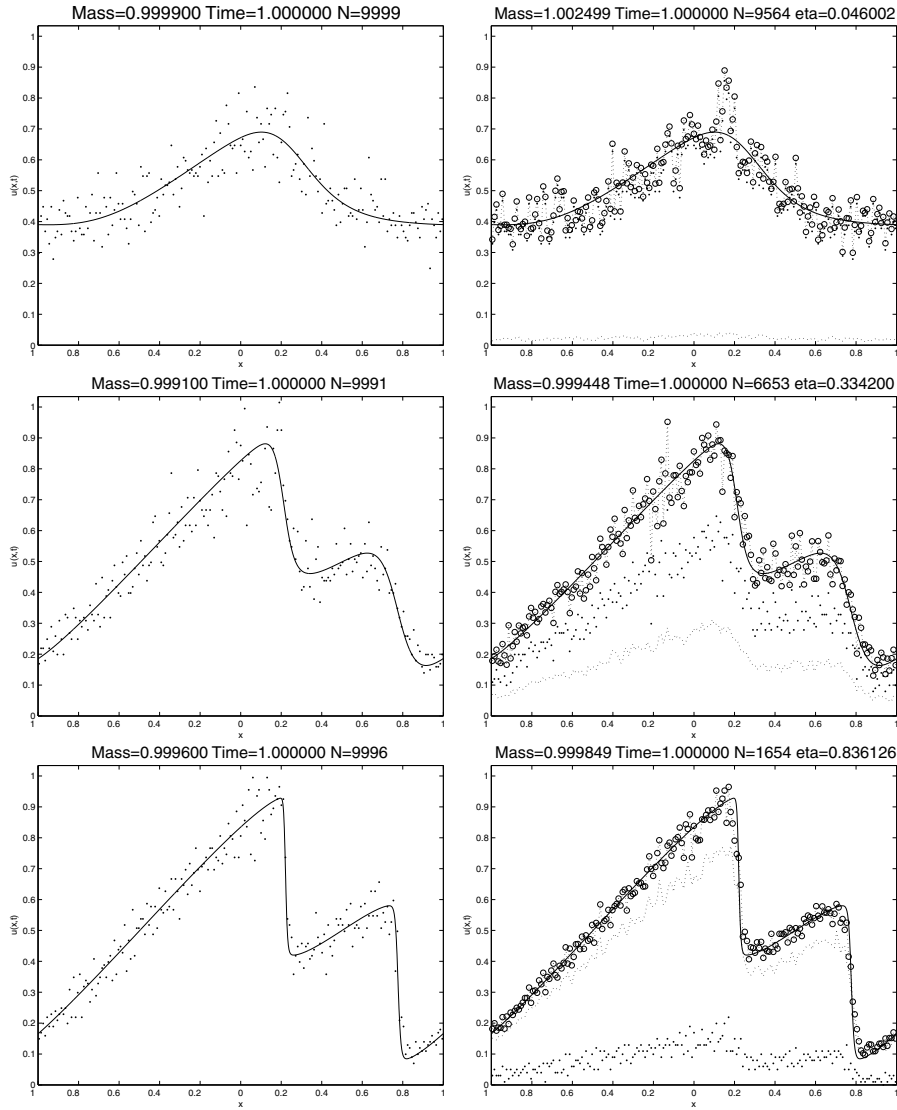


FIG. 4.1. 1D case: Solution at  $t=1$  with  $\varepsilon=0.1$  (top),  $\varepsilon=0.01$  (middle) and  $\varepsilon=0.001$  (bottom) for MCM (left) and HM1 (right), with initial data (4.3). Particle solution ( $\cdot$ ), equilibrium solution (dashed line) and hybrid solution ( $\circ$ ). The solid line represents a fully resolved numerical solution.

#### 4.2.2. 2D case.

Next we consider the 2D case

$$\begin{aligned}
 \partial_t u + \partial_x v + \partial_y w &= 0, \\
 \partial_t v + \partial_x p(u) &= -\frac{1}{\varepsilon}(v - F(u)), \\
 \partial_t w + \partial_y q(u) &= -\frac{1}{\varepsilon}(w - G(u)),
 \end{aligned} \tag{4.4}$$

with  $F(u) = G(u) = u^2/2$ . For  $\varepsilon \rightarrow 0$  we obtain the 2D Burgers equation

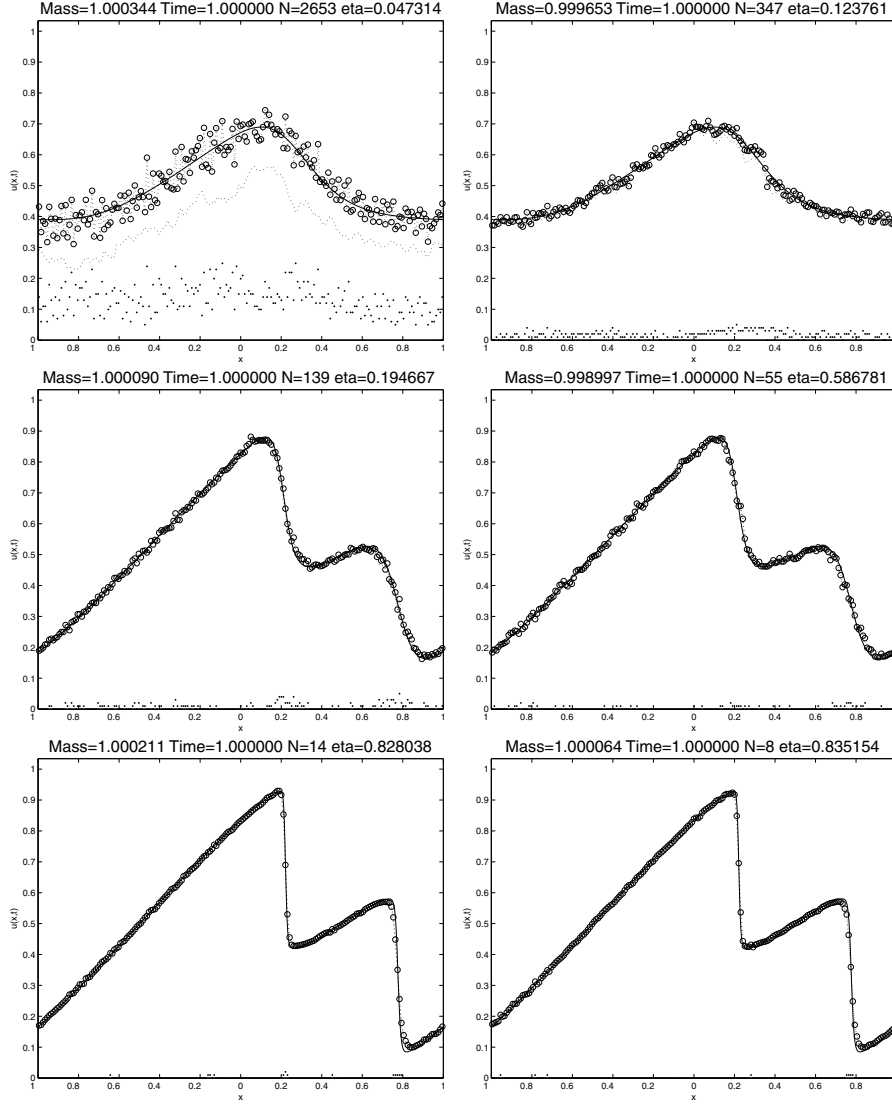


FIG. 4.2. 1D case: Solution at  $t=1$  with  $\varepsilon=0.1$  (top),  $\varepsilon=0.01$  (middle) and  $\varepsilon=0.001$  (bottom) for HM2 (left) and CHM (right), with initial data (4.3). Particle solution ( $\cdot$ ), equilibrium solution (dashed line) and hybrid solution ( $\circ$ ). The solid line represents a fully resolved numerical solution.

$$\partial_t u + \partial_x \frac{u^2}{2} + \partial_y \frac{u^2}{2} = 0. \quad (4.5)$$

We consider periodic boundary conditions and initial data

$$u(x, y) = \sin(\pi x)^2 \sin(\pi y)^2, \quad (x, y) \in [0, 1]^2.$$

First we report the result for the three hybrid methods for  $\varepsilon=0.1$  and  $\varepsilon=0.01$  using a  $40 \times 40$  mesh. The initial data is represented by  $N=8 \times 10^4$  particles. The

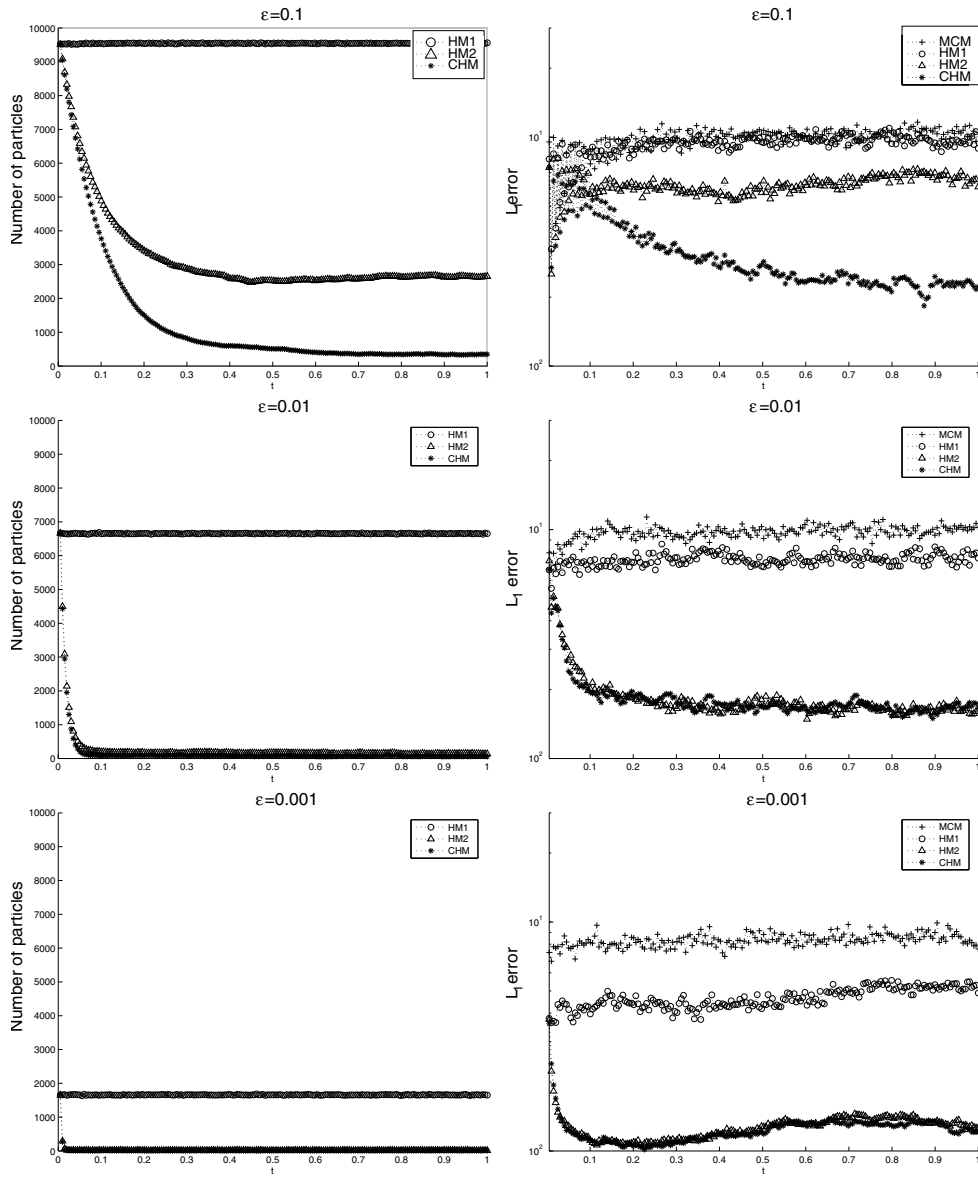


FIG. 4.3. 1D case: Number of particles (left) and relative  $L_1$ -error in time (right) for  $\epsilon=0.1$  (top),  $\epsilon=0.01$  (middle) and  $\epsilon=0.001$  (bottom), for (4.3) initial data.

results and the final computation times are shown in Figure 4.4 for  $\epsilon=0.1$  and in Figure 4.5 for  $\epsilon=0.01$ . We omit the results for the HM2 method since they are very similar to the results of CHM.

Finally we also report the result obtained for  $\epsilon=10^{-6}$  with a  $80 \times 80$  mesh (Figure 4.6). In this latter case, due to the small value of  $\epsilon$  all hybrid methods yield essentially the same result corresponding to the second order relaxation scheme for the limiting equation.

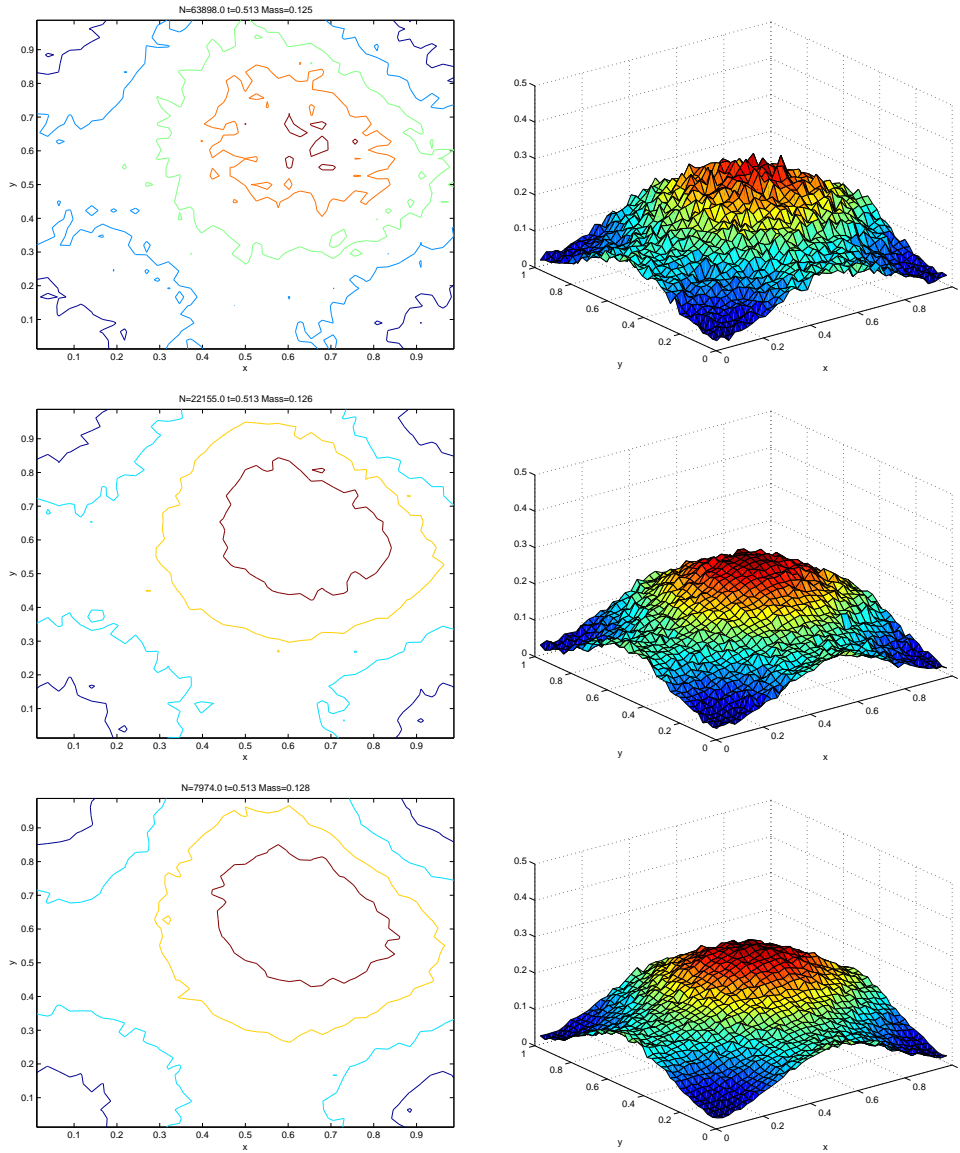


FIG. 4.4. 2D case: Solution at  $t=0.5$  with  $\varepsilon=0.1$  for MCM (top) HM1 (middle) and CHM (bottom).

**4.3. Broadwell models.** The extension of the above schemes to the case of the Broadwell model equations does not present any particular difficulty and we omit the details. We solve the Broadwell equations with  $\alpha = 1$ , corresponding to the four velocity reduced Broadwell models, with the following initial data

$$\rho(x,0) = 2 \quad m = 1 \quad z = 1 \quad x < 0,$$

$$\rho(x,0) = 1 \quad m = 0.13692 \quad z = 1 \quad x > 0.$$

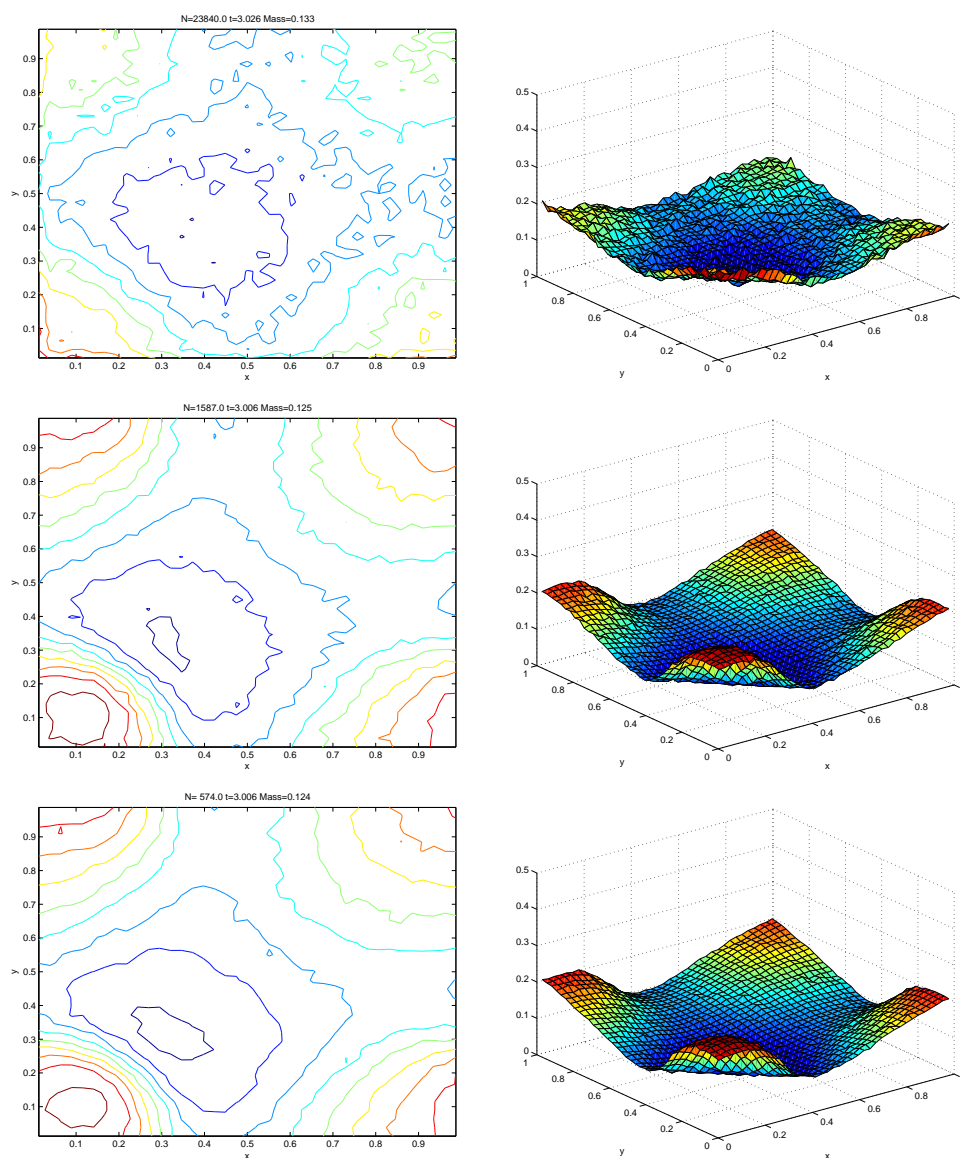


FIG. 4.5. 2D case: Solution at  $t=3$  with  $\varepsilon=0.01$  for MCM (top) HM1 (middle) and CHM (bottom).

We integrate over the domain  $[-1,1]$  with a reflecting boundary condition. We use 100 grid points for  $\varepsilon=1$  and  $\varepsilon=0.02$  and 200 grid points for  $\varepsilon=0.001$  starting initially with  $N=3 \times 10^3$  particles. The reference solution is obtained using a second order finite difference solver with six times the cells number of the computed hybrid solution.

We report the results obtained with the different hybrid methods and the Monte Carlo method (MCM) depicted with the reference solution. Note that the initial datum for  $z$  is not a local equilibrium, which yields an initial layer. First we consider the case  $\varepsilon=1$  ( Figure 4.7) corresponding to a non-stiff (rarefied) regime where all

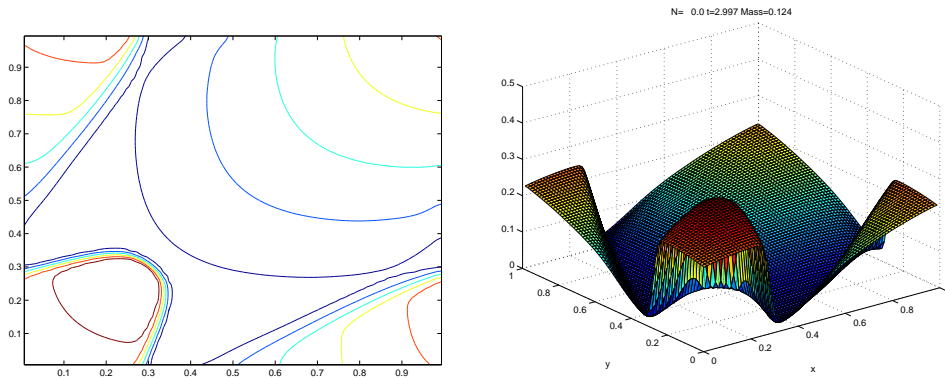


FIG. 4.6. 2D case: Solution at  $t=3$  with  $\varepsilon=10^{-6}$  for HM methods.

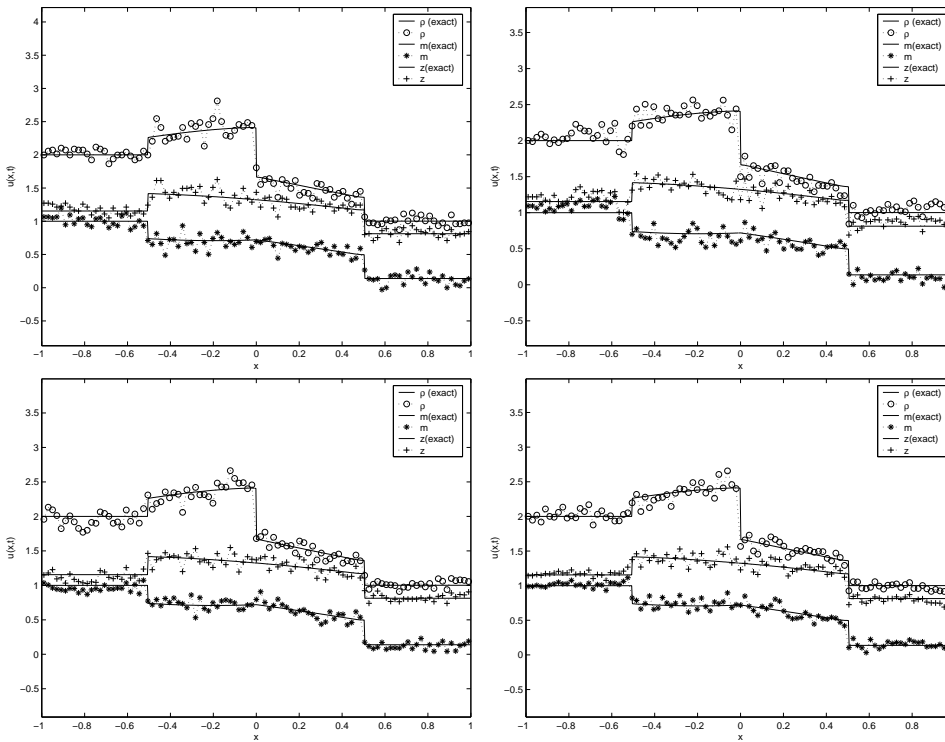


FIG. 4.7. The numerical solutions of Broadwell equations for  $\rho=(\circ)$ ,  $m=(+)$  and  $z(*)$  with MCM (top left) HM1 (top right) HM2 (bottom left) CHM (bottom right) for  $\varepsilon=1$ . The solid line represents a fully resolved numerical solution.

the hybrid methods give a very similar result to MCM. In fact, we are far from the local thermal equilibrium and the solution is represented mostly by samples in all schemes. In the intermediate regime ( Figure 4.8, where  $\Delta x$ ,  $\Delta t$  and  $\varepsilon$  are of the same order, the methods give different results, in particular HM1 is very close to MCM, whereas HM2 and CHM provide a more accurate solution with fewer fluctuations

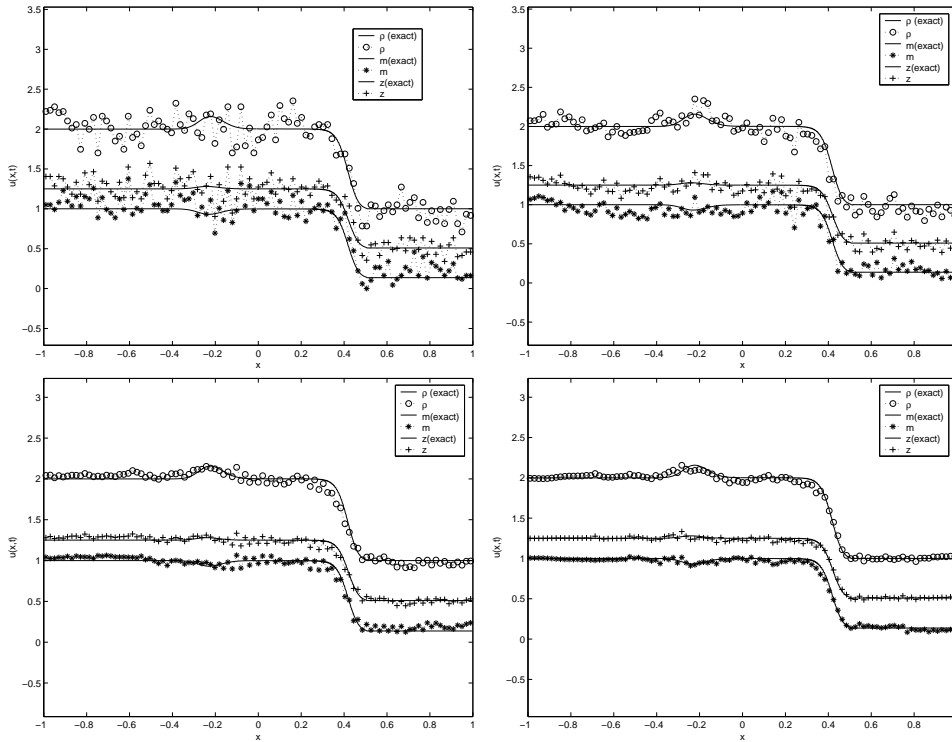


FIG. 4.8. The numerical solutions of Broadwell equations for  $\rho=(\circ)$ ,  $m=(+)$  and  $z(*)$  with MCM (top left) HM1 (top right) HM2 (bottom left) CHM (bottom right) for  $\varepsilon=0.02$ . The solid line represents a fully resolved numerical solution.

due to the stochastic component of the solution. The small hump that is possible to notice near  $x=-0.2$  is part of the exact solution. It is due to the fact that the initial condition represents an exact traveling shock wave for the relaxed system. Finally we consider the stiff regime  $\varepsilon=10^{-6}$  (Figure 4.9), corresponding to the Euler limit where the solution is a shock wave moving right with speed  $s=0.86038$  determined by the Rankine-Hugoniot jump condition. In this latter case all hybrid methods give essentially the same result due to the high resolution second order deterministic solver.

## 5. Conclusion

In this paper we have considered the development of hybrid methods for multiscale problems. Here we restricted our analysis to the case of hyperbolic systems with relaxation. The general methodology is based on a suitable blending of particle representation of the non-equilibrium part of the solution with a finite difference or finite volume approximation of the equilibrium part. In order to better explain the structure of the schemes we considered applications to simple relaxation systems. Several numerical results show the efficiency of the schemes and their ability to merge correctly the probabilistic and the deterministic fraction of the solution. The schemes here presented rely on a relaxed scheme as deterministic solver and on a kinetic-like interpretation of the hyperbolic system for the Monte Carlo solver. In summary we can say that all hybrid methods presented here have better computational efficiency and accuracy properties of a full particle solver. The gain in efficiency and accuracy

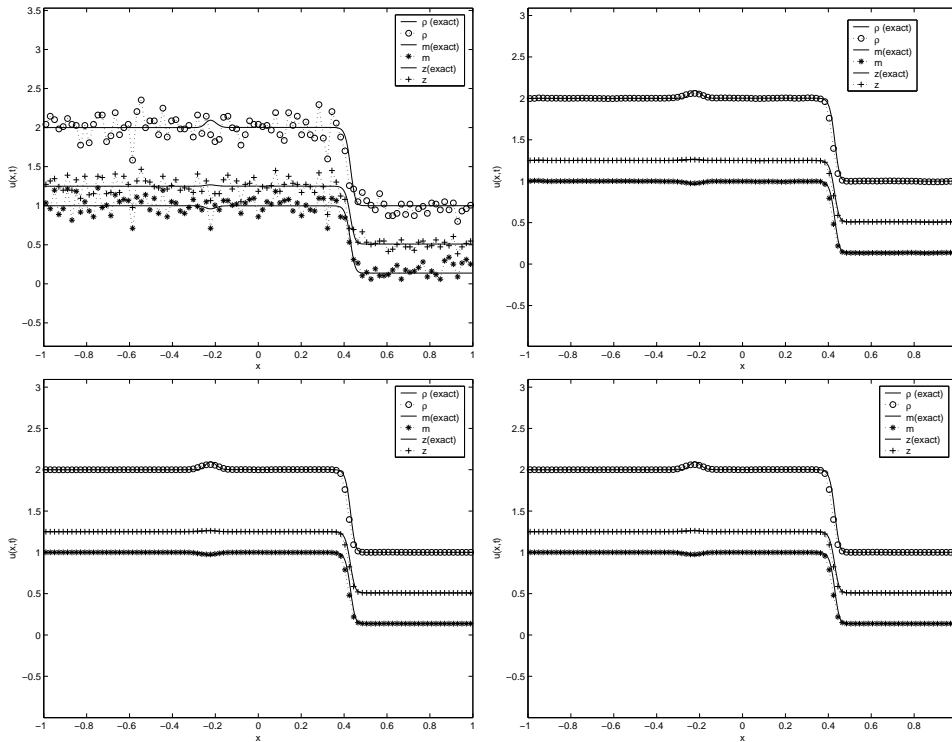


FIG. 4.9. The numerical solutions of Broadwell equations for  $\rho=(\circ)$ ,  $m=(+)$  and  $z(*)$  with MCM (top left) HM1 (top right) HM2 (bottom left) CHM (bottom right) for  $\varepsilon=10^{-6}$ . The solid line represents a fully resolved numerical solution.

is inversely proportional to the relaxation parameter  $\varepsilon$ . Among hybrid methods, the HM2 scheme, due to its generality, represents the most promising method for realistic applications.

Several interesting questions remain open among which we mention:

- Inclusion in the schemes of a more general fluid solver.
- Extension of the present methods to kinetic equations and other multiscale problems such as diffusive limits.
- Convergence and error estimates for the hybrid schemes.

Finally let us mention that the examples presented here refer to unsteady problems. In many applications (for example in kinetic theory) the problems are mostly steady state. Similarly to Monte Carlo methods, suitable averaging procedures in time on the stochastic fraction of the hybrid methods may be used in such cases to speed up convergence.

The prospects in these directions are encouraging and we hope to present more challenging results in the near future [9].

**Acknowledgements.** The authors would like to thank Russ Caflisch for the many stimulating discussions.

## REFERENCES

- [1] J. F. Bourgat, P. LeTallec, B. Perthame and Y. Qiu, *Coupling Boltzmann and Euler equations without overlapping*, in Domain Decomposition Methods in Science and Engineering, Contemp. Math. 157, AMS, Providence, RI, 377-398, 1994.
- [2] J. E. Broadwell, *Shock structure in a simple discrete velocity gas*, Phys. Fluids, 7, 1013-1037, 1964.
- [3] R. E. Caflisch, *Monte Carlo and quasi-Monte Carlo methods*, Acta Numerica, 1-49, 1998.
- [4] R. E. Caflisch, S. Jin and G. Russo, *Uniformly accurate schemes for hyperbolic systems with relaxation*, SIAM J. Numer. Anal., 34, 246-281, 1997.
- [5] R. E. Caflisch and E. Luo, *A uniform hybrid Monte Carlo method for simulation of rarefied gas dynamics*, preprint, 2004.
- [6] C. Cercignani, R. Illner and M. Pulvirenti, *The Mathematical Theory of Dilute Gases*, Springer-Verlag, New York, 1995.
- [7] G. Q. Chen, D. Levermore and T. P. Liu, *Hyperbolic conservation laws with stiff relaxation terms and entropy*, Comm. Pure Appl. Math., 47, 787-830, 1994.
- [8] N. Crouseilles, P. Degond and M. Lemou, *A hybrid kinetic-fluid model for solving the gas-dynamics Boltzmann BGK equation*, J. Comp. Phys., 199, 776-808, 2004.
- [9] G. Dimarco and L. Pareschi, *Hybrid multiscale methods II. Kinetic equations*, work in progress, 2005.
- [10] W. E and B. Engquist, *The heterogeneous multiscale methods*, Comm. Math. Sci., 1, 87-133, 2003.
- [11] W. E and B. Engquist, *The heterogeneous multiscale method for homogenization problems*, Multiscale Methods in Science and Engineering, Lect. Notes Comput. Sci. Eng., 44, 89-110, 2005.
- [12] W. E and B. Engquist, *Multiscale modeling and computation*, Notices of the AMS, 50(9), 1062-1070, 2003.
- [13] E. Gabetta, L. Pareschi and G. Toscani, *Relaxation schemes for nonlinear kinetic equations*, SIAM J. Numer. Anal., 34, 2168-2194, 1997.
- [14] S. Jin, C. D. Levermore, *Numerical schemes for hyperbolic conservation laws with stiff relaxation terms*, J. Comp. Phys., 126, 449-467, 1996.
- [15] S. Jin, L. Pareschi and G. Toscani, *Diffusive relaxation schemes for multiscale discrete-velocity kinetic equations*, SIAM J. Numer. Anal., 35, 2405-2439, 1998.
- [16] S. Jin, L. Pareschi and G. Toscani, *Uniformly accurate diffusive relaxation schemes for multiscale transport equations*, SIAM J. Numer. Anal., 35, 2405-2439, 1998.
- [17] S. Jin and Z. P. Xin, *Relaxation schemes for systems of conservation laws in arbitrary space dimensions*, Comm. Pure Appl. Math., 48, 235-276, 1995.
- [18] M. A. Katsoulakis, A. J. Majda and A. Sopsakis, *Multiscale couplings in prototype hybrid deterministic/stochastic systems: part I, Deterministic Closures*, Comm. Math. Sci., 2, (2), 255-294, 2004.
- [19] P. LeTallec and F. Mallinger, *Coupling Boltzmann and Navier-Stokes by half fluxes*, J. Comp. Phys., 136, 51-67, 1997.
- [20] R. J. LeVeque, *Numerical Methods for Conservation Laws*, Lectures in Mathematics, Birkhauser Verlag, Basel, 1992.
- [21] S. Liu, *Monte Carlo Strategies in Scientific Computing*, Springer, 2004.
- [22] T.-P. Liu, *Hyperbolic conservation laws with relaxation*, Comm. Math. Phys., 108, 153-175, 1987.
- [23] G. Naldi and L. Pareschi, *Numerical schemes for hyperbolic systems of conservation laws with stiff diffusive relaxation*, SIAM J. Numer. Anal., 37, 1246-1270, 2000.
- [24] R. Natalini, *Convergence to equilibrium for relaxation approximations of conservation laws*, Comm. Pure Appl. Math. 49, 795-823, 1996.
- [25] L. Pareschi, *Central differencing based numerical schemes for hyperbolic conservation laws with stiff relaxation terms*, SIAM J. Num. Anal., 39, 1395-1417, 2001.
- [26] L. Pareschi and R. E. Caflisch, *Implicit Monte Carlo methods for rarefied gas dynamics I: the space homogeneous case*, J. Comp. Phys., 154, 90-116, 1999.
- [27] L. Pareschi and R. E. Caflisch, *Towards an hybrid method for rarefied gas dynamics*, IMA Vol. App. Math., 135, 57-73, 2004.
- [28] L. Pareschi, *Hybrid multiscale methods for hyperbolic and kinetic problems*, ESAIM: PROCEEDINGS, T. Goudon, E. Sonnendrucker & D. Talay, Editors, 15, 87-120, 2005.
- [29] L. Pareschi and M. Seaid, *A new Monte Carlo approach for conservation laws and relaxation systems*, Lecture Notes in Computer Science, 3037, 281-288, 2004.
- [30] R. Roveda, D. B. Goldstein and P. L. Varghese, *Hybrid Euler/direct simulation Monte Carlo*

- calculation of unsteady slit flow*, AIAA J. Spacecraft Rockets 37, 753-760, 2000.
- [31] T. Schulze, P. Smereka and W. E, *Coupling kinetic Monte-Carlo and continuum models with application to epitaxial growth*, J. Comp. Phys., 189, 197-211, 2003.